Learning with Muscles: Benefits for Data-Efficiency and Robustness in Anthropomorphic Tasks

Anonymous Author(s)
Affiliation
Address
email

Abstract: Humans are able to outperform robots in terms of robustness, versatility, and learning of new tasks in a wide variety of movements. We hypothesize that highly nonlinear muscle dynamics play a large role in providing inherent stability, which is favorable to learning. While recent advances have been made in applying modern learning techniques to muscle-actuated systems both in simulation as well as in robotics, so far, no detailed analysis has been performed to show the benefits of muscles in this setting. Our study closes this gap by investigating core robotics challenges and comparing the performance of different actuator morphologies in terms of data-efficiency, hyperparameter sensitivity, and robustness [1].

Keywords: reinforcement learning, model predictive control, actuator morphology, morphological computation

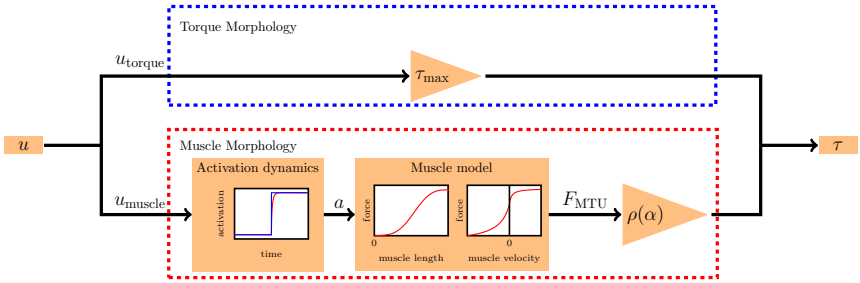

Figure 1: Key differences between torque actuator morphology and muscle actuator morphology.

1 Introduction

Recent developments in new learning methods allow the generation of complex anthropomorphic motions in robotics. However, current systems still struggle with real-world scenarios beyond the narrow conditions of laboratory experiments. Humans, on the other hand, are capable of quickly adapting to uncertain, complex, and changing environments in a sheer endless variety of tasks. One key difference between biological and robotic systems lies in their actuator morphology: robotic drives are mostly designed to yield a linear relation between control signal and output torque. In contrast, muscles have complex nonlinear characteristics.

It has already been demonstrated, that muscular nonlinearities may provide a benefit for stability and robustness, especially under environmental uncertainties or perturbations [1, 2, 3]. A benefit over linear torque actuator morphology has been observed in computer simulations by exchanging the actuator morphology in otherwise identical anthropomorphic tasks like reaching [4] or locomotion [5, 6, 7, 8]. Similarly, reduced demand on the information processing capacity has been shown for

[1] See https://sites.google.com/view/learning-with-muscles for videos.

Submitted to the 6th Conference on Robot Learning (CoRL 2022). Do not distribute.

muscles when compared to torque actuator morphology [9, 10, 11, 12, 13]. This opens the question whether muscular morphology could also be beneficial for robustness and data-efficiency in the process of *learning* movement control.

Recent advances in deep learning facilitated the generation of complex movements like point-reaching [14, 15, 16, 17] and locomotion [18, 19, 20, 21, 17] in simulations with muscular actuator morphology. In the real world, optimization and learning approaches can also find controllers for robotic systems with pneumatic muscles exhibiting somewhat muscle-like actuator morphology [22, 23]. These examples demonstrate that learning and optimization methods *can* control muscle-driven systems and may enable benefits such as safe learning and robustness [23]. However, investigating advantages of nonlinear muscular actuator morphology over linear torque actuator morphology requires a direct comparison of both, which is—to our knowledge—missing in the literature.

The purpose of this study is to test if learning with muscular actuator morphology is more data-efficient and results in more robust performance as compared to torque actuator morphology. We investigate this in a very broad approach: we employ different learning strategies on multiple anthropomorphic models for multiple variants of reaching and locomotion tasks solved in physics simulators of differing levels of detail. This provides new and comprehensive evidence of the beneficial contribution of muscular morphology to the learning of diverse movements.

2 Morphological difference between torque and muscle actuators

In contrast to idealized torque actuators, where torque is simply proportional to the control signal $u_{\text{torque}} \in [-1, 1]$,

$$\tau = \tau_{\text{max}}\, u_{\text{torque}} \tag{1}$$

muscular force output nonlinearly depends on the muscle control signal u_{muscle}, the muscle length l_{MTU} and contraction velocity $\dot{l}_{\text{MTU}}$. These biologically observed dependencies can be predicted by so-called *Hill-type* muscle models [24]. In a nutshell, the model captures biochemical processes transforming muscle stimulation $u_{\text{muscle}} \in [0, 1]$ to the force-generating calcium ion activity a. This can be modeled by a first-order differential equation of the form [25]

$$\dot{a} = f_a(u_{\text{muscle}} - a) \tag{2}$$

which induces low-pass filter characteristics (Fig. 1). The model further captures the nonlinear *force-length* and *force-velocity relations* [24]. The *force-length relation* is characterized by a positive slope (increasing force with increasing muscle fiber length) in the typical operating range of biological muscle fibres (Fig. 1). The *force-velocity* relation is characterized by decreasing force for faster shortening velocities and increasing force if the muscle is externally stretched against its contraction direction (Fig. 1). A lever arm $\rho(\alpha)$ translates joint angle α into muscle-tendon-unit length l_{MTU} and muscle force into joint torque

$$\tau = \sum_{i=1}^{N} \rho_i(\alpha) f_\tau \left(l_{\text{MTU},i}(\alpha), \dot{l}_{\text{MTU},i}(\dot{\alpha}), a_i \right). \tag{3}$$

for N muscles which span a joint—typically at least two in an antagonistic arrangement.

In practice, we employ two different muscle models: A detailed one with more physiological details, contained in demoa [26], and a simpler model that efficiently adds muscular properties to existing MuJoCo [27] simulations without sacrificing computational speed. See Suppl. A for details.

3 Methods

3.1 Learning approaches for movement control

We test if muscle actuator morphology facilitates learning by applying state-of-the-art learning algorithms covering an extensive range of approaches currently used in robotics. The common thread

Table 1: **Overview of all models and tasks**

Model	Task	Control	Environment
ArmMuJoCo	precise reaching	RL	MuJoCo
ArmMuJoCo	fast reaching	RL	MuJoCo
ArmDemoa	smooth point-reaching	opt. control, MPC	demoa
ArmDemoa	hitting ball with high-velocity	opt. control, MPC	demoa
Biped	hopping	RL	MuJoCo
FullBody	squatting	opt. control, MPC	demoa
FullBody	high-jumping	opt. control, MPC	demoa

(a) ArmMuJoCo (b) ArmDemoa (c) Biped (d) FullBody

Figure 2: Models used for the experiments.

of the selected algorithms lies in their independence of the actuator morphology: this allows us to easily exchange idealized torque actuator morphology with muscle actuator morphology. We choose optimal control, model-predictive control and reinforcement learning as learning approaches.

Optimal control (OC) The control problem with horizon N can be defined as:

$$\min_{\pi_k} J = \min_{\pi_k} \sum_{k=0}^{N} l(x(k), u(k), k), \qquad \text{subject to } \; x(k+1) = f(x(k), u(k), k),$$
$$u(k) = \pi_k(x(0), ..., x(k)). \tag{4}$$

where $x(k) \in \mathbb{R}^{n_x}$ denotes the current state at time k, and $u(k) \in \mathbb{R}^{n_u}$ is the applied input at time k. Furthermore, l specifies the cost function, and f denotes the system dynamics. To optimize for the best control policy, we use the covariance matrix adaptation evolution strategy (CMA-ES) [28] in the optimal control case (open-loop strategy). CMA-ES is a derivative-free algorithm and widely used in machine learning. It combines different learning mechanisms for adapting the parameters of a multivariate normal distribution. Note, that we choose the same optimization parameters for both actuator morphologies to allow for a fair comparison even though the number of decision variables n_u is always larger in the muscle-actuated case due to the antagonistic setup.

Model predictive control (MPC) In MPC, we solve the control problem in a receding-horizon fashion with varying prediction horizons and recursively apply only the first element of the predicted optimal control sequence $u(0)$ (closed-loop strategy). We employ a warm start procedure using the CMA-ES optimizer and afterwards start the MPC routine with the local optimizer BOBYQA [29]. The parameters of the optimizers are either varied (see Sec. 4) or given in Suppl. B

Reinforcement learning (RL) RL allows learning of reusable feedback controllers. Instead of *minimizing* a cost function (see Eq. 4), conventionally the discounted expected reward is *maximized*:

$$\max_{\pi} J = \max_{\pi} \mathbb{E}\left[\sum_{k=0}^{N-1} \gamma^{k-1}\, r(k)\right] \tag{5}$$

where $r(k)$ is the reward at time k, π is a control policy and $\gamma \in [0, 1]$ is a discount factor such that long-term rewards are weighted less strongly. RL consequently solves a similar problem to MPC, but the resulting controllers are able to act in closed-loop fashion without being given an explicit prediction model. For the point-reaching tasks, we additionally employ goals g characterizing the

desired hand position, which then constitutes an additional dependence of the reward function. The aim of the learning process is to learn a controller policy $\pi(u(k)|x(k))$ that takes as input the current sensor values, or state x(k), and outputs a control signal, or action, $u(k)$ such that a task is solved. In practice, we use the RL algorithm MPO [30], implemented in TonicRL [31].

3.2 Models

Arm The Arm model (Fig. 2 a, b) consists of two segments connected with hinge joints (2 joints total) moving against gravity. The ArmMuJoCo [27, 17] model contains four muscles, two for each joint. In the muscle-actuated case in ArmDemoa [32, 33], six Hill-Type muscles generate forces: two muscles for the shoulder and two for the elbow joint, plus two biarticular muscles acting on both joints. All joints are individually controllable.

Biped We converted the geometrical model of an OpenSim bipedal human without arms [19] for use in MuJoCo. The model, consisting of 7 controllable joints (lower back, hips, knees, ankles) moves in a 2D plane. Each joint is actuated by two antagonistic muscles or one torque actuator.

FullBody The FullBody model [34, 35] consists of two legs and an upper body including arms based on a human skeletal geometry. It consists of 8 controllable joints (ankles, knees, hips, lumbar and cervical spine) in 3D, and 14 movable joints in total including the arms. Each controllable joint was either actuated by two antagonistic muscles (muscle-actuated case) or by one idealized torque actuator (torque-actuated case). For more details, we refer to Suppl. C.

3.3 Objectives and rewards

We choose anthropomorphic movement objectives which are highly relevant for robotic applications. We expect that muscular actuator morphology provides benefits for such tasks. All task formulations allow application in muscle and torque actuator morphologies with an identical reward or objective function. For a precise formulation of the used functions and conditions, see Suppl. D.

Smooth point-reaching This task encourages *smooth* point-reaching. Therefore, the objective minimizes the L2-error between the desired and current joint angle while penalizing the angle velocity and jerk to ensure a smooth motion. The desired angle is $90°$ for both the shoulder and the elbow joint, as this requires a large motion.

Precise point-reaching Similar to [13], we incentivize reaching a random hand position in a predetermined rectangle, while minimizing the distance of the end effector to the goal. We specifically add a reward term that gives a much larger reward for precise motions that reach the center of the target area. The episode does not terminate until a time limit of 1000 steps elapses.

Fast point-reaching The same objective as for precise point-reaching is used, but the episode terminates if the target is reached, incentivizing reaching speed over precision.

High-velocity ball serve A ball is dropped in front of the Arm model and the controller learns to hit the ball to achieve maximum ball velocity.

Squatting This squatting objective is taken from [34] and encourages desired hip, knee, and ankle angles for a squatting position.

Maximum height jump The objective for the high-jumping task is taken from [36] and maximizes the position and velocity of the centre of mass of the human body model at the time of lift-off. The model is initialized to start from a squatting position.

Hopping We developed an objective based on the z-axis velocity of the center of mass (COM) of the system that encourages periodic hopping with maximum height. The episode terminates if extreme joint angles are exceeded.

4 Results

In the following, we present three major results for the investigated approaches and environments: (**1**) Muscle-like actuators in general improve data-efficiency compared to torque-actuators. (**2**) The investigated learning and optimization algorithms exhibit greater robustness to hyperparameter

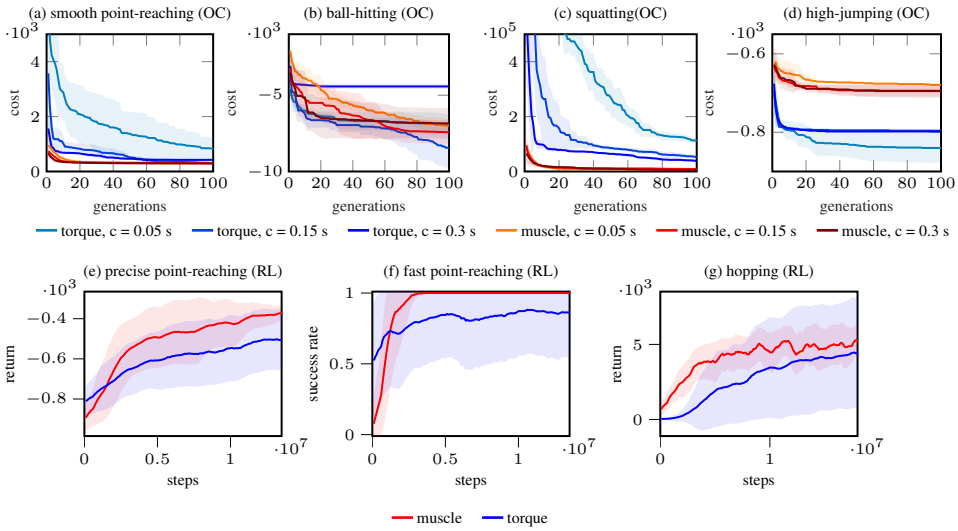

Figure 3: **Cost value or returns for different tasks.** Plotting the mean and standard deviation (shaded area) for 5 (OC/MPC) or 8 (RL) repeated runs for the two actuator morphologies (muscle in red, torque in blue).

variations when applied to muscle-driven systems. (**3**) The motions and controllers obtained from the muscular morphology are more robust against force perturbations that were not present during learning. We average results over 5 and 8 random seeds for OC/MPC and RL respectively.

4.1 Data efficiency: Learning with limited resources

Robotics applications in real-world scenarios often suffer from limited resources, which holds true for training and inference time. Therefore, we investigate the advantages of muscle-like actuator morphology in terms of overall learning efficiency and temporal control resolution.

Advantages of muscular morphology Smooth and precise point-reaching generally require more data with torque-driven systems, as seen in Fig. 3. The performance of the muscle actuator, in contrast to torque morphology, varies very little for different settings of the temporal control resolution c. Precise reaching with RL also results in stable performance with fewer training iterations, and a very small standard deviation across runs. Similar findings are seen for the squatting and hopping task, where muscle-actuators achieve better data-efficiency and smaller variation across runs and are able to find a good-enough optimum with fewer iterations.

Advantages of torque morphology In tasks requiring fast and strong motions, without emphasis on stabilization, we find torque actuators to hold certain advantages. In ball hitting and fast reaching, the torque cases show similar or smaller variance, even though both actuators perform well for singular runs. The high-jumping task, where only a strong, swift motion is required to launch the system upwards, is solved much faster in the torque case. We can also observe in the hopping task that, although only after a considerable number of training iterations and exhibiting a large variance, some torque-actuated runs achieve a larger overall return than the best muscle-actuated runs.

4.2 Robustness to hyperparameter variations

Tuning a growing number of hyperparameters for learning models typically requires considerable time and computational resources. By analysing hyperparameter sensitivity, we test if tuning with torque or muscle actuator morphologies requires less resources.

Figure 4 shows the cost curves for smooth point-reaching for the evolutionary optimization algorithm CMA-ES for different values of σ, which is the principal tuneable parameter for this algorithm. The performance curves vary much stronger for torque actuators for all considered cases. Furthermore,

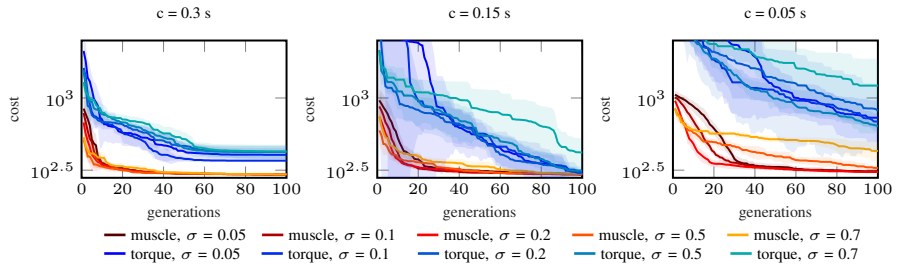

Figure 4: **Muscle morphology is more robust towards hyperparameter variation (σ) in point reaching.** The cost value of the best observation is shown. The mean and standard deviation (shaded area) are plotted for five repeated runs for the two actuator morphologies (muscle in red, torque in blue) with different control resolutions c.

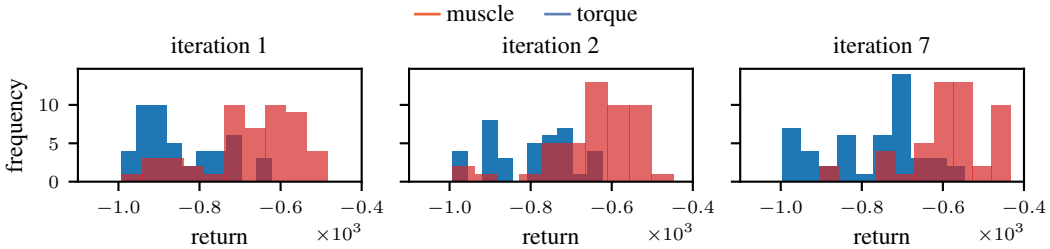

Figure 5: **Muscle actuators need less parameter tuning for good performance.** Hyperparameters are optimized for precise point-reaching following an iterative sampling scheme, each run trains for 2×10^6 iterations. Fifty sets of parameters are sampled randomly from pre-determined distributions, the final performance is evaluated and used to adapt the sampling distributions for the next iteration. We plot the return distributions over the sampled parameters at different iterations.

all muscle-actuated cases find a good-enough optimum with fewer iterations and a smaller variance, independent of the hyperparameter σ and the control resolution c.

The same task was repeated using MPC while varying the main hyperparameter t_{pred}, which represents the prediction horizon in moving horizon strategies. The performance curves and the final cost vary much stronger for torque actuators (Fig. 6a, note, the cost is plotted logarithmically).

Finally, we performed an extensive hyperparameter optimization for precise point-reaching. For each iteration, 50 sets of parameters are randomly chosen and the final task performance is evaluated after 2×10^6 learning iterations. The sampling distributions for the parameters are then fit to the best performing runs and 50 additional sets are evaluated for the next iteration. We optimize the learning rates of MPO, as well as gradient-clipping thresholds, as these have a strong influence on learning speed and stability. Muscle actuators already outperform torque-actuators in the first iteration, with a greater number of well performing parameter sets (Fig. 5). Almost no low-performing runs remain for iteration 7, while a large torque-performance is only achieved by a small subset of parameter settings. See Suppl. E for more hyperparameter variations.

4.3 Robustness to perturbations

In this section, we probe the robustness of the obtained policies against unknown perturbations. In precise point-reaching, we evaluated the RL reaching policies for two modifications that were not present during training: First, the hand-weight of the model is increased by 1.5 kg (dynamic load), and secondly a free spherical weight is attached to the end effector with a cable (chaotic load). We can see in Fig. 8 that the muscle-based policy does not suffer significant changes in performance, except for a small circular motion (3 cm) around the goal position in the chaotic load case. In contrast, the torque actuator morphology leads to unstable reaching and strong oscillations. Both morphologies seem to handle the dynamic load well. See Suppl. E for more goals.

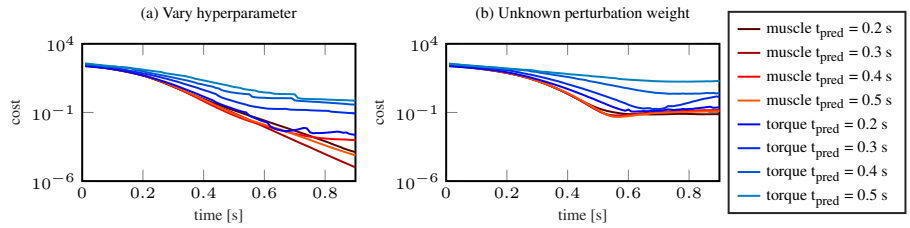

Figure 6: **Muscle morphology is more robust towards variation of hyperparameter t_{pred} and unknown perturbations.** Plotting the development of cost over time for the two actuator morphologies (muscle in red, torque in blue) while varying the hyperparameter t_{pred} denoting the length of the prediction horizon. Left: The unperturbed case. Right: The prediction model is not aware of the added weight to the lower arm.

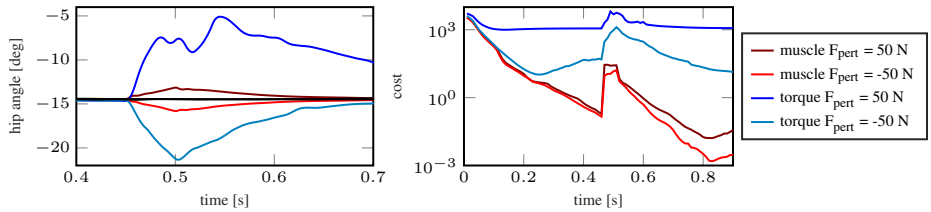

Figure 7: **Hip and cost trajectory for squatting with unknown perturbation forces.** The muscle morphology is shown in red, the torque morphology in blue while varying the perturbation force F_{pert} [N] (applied between $t >= 0.45$ s and $t <= 0.5$ s).

For the MPC controller, we evaluated robustness by introducing environment changes that are unknown to the prediction model. One example is the lifting of an object with unknown weight, a typical robotics task. When adding 1 kg to the lower arm of the ArmDemoa model (Fig. 6), the performance in both actuator cases is worse than in the unperturbed case (left); the movement is also slower. However, the variance and absolute value of the final cost in the muscle-actuated case are still much lower compared to the torque-actuated case (plotted logarithmically).

For periodic hopping with the Biped model, we evaluated trained RL policies with random forces that were drawn from a Gaussian distribution $F \sim \mathcal{N}(\cdot|0, \sigma_F)$ and applied to the hip, knee, and ankle joints with a probability of 0.05 at each time step. We see in Fig. 9 that the torque actuator morphology is stronger affected in relative performance than the muscle morphology. In the robustness investigation with MPC in the FullBody squatting task, a force is applied to the hip joint after the system has reached its desired position. Figure 7 (left) shows that the desired joint angles are much less affected by the perturbation when muscle actuators are controlled. Furthermore, the cost value associated with the movement recovers much slower for torque actuators (Fig. 7 right).

5 Discussion

We investigated if muscle-like actuators have beneficial effects for modern learning methods in terms of data-efficiency, hyperparameter sensitivity and robustness to perturbations. A multitude of variations across physics simulators, learning algorithms and task domains was considered in order to showcase the potential of the considered morphologies independently of the underlying implementation. We showed that muscles yield benefits in tasks requiring stable motion, even when compared to idealized torque actuators, which can be considered an upper performance bound. Indeed, the used torque actuators are able to instantaneously output any desired force at any point of the trajectory, while muscles only slowly change their output due to activation dynamics and can only produce kinematics-dependant force output. Despite these limitations, the considered learning algorithms learn more efficiently with muscle actuation in all tasks, except for extreme motions where objectives require a strong force application without stability considerations, such as ball-hitting

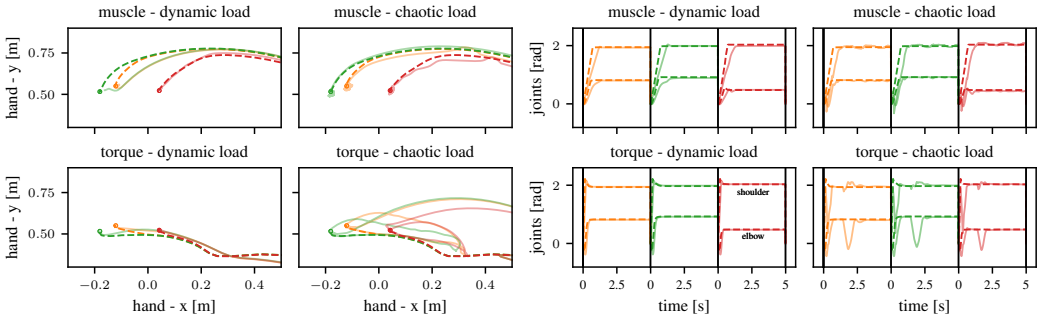

Figure 8: **Trajectories for dynamic (1.5 kg weight) and chaotic (attached ball) load.** Left: Three random goals are exemplarily shown, the respective goal position is marked as a circle. The unperturbed baseline for each goal is shown with a dashed line. Right: Joint trajectories for the same experiment, the unperturbed baselines are shown with dashed lines. Vertical bars mark episode resets.

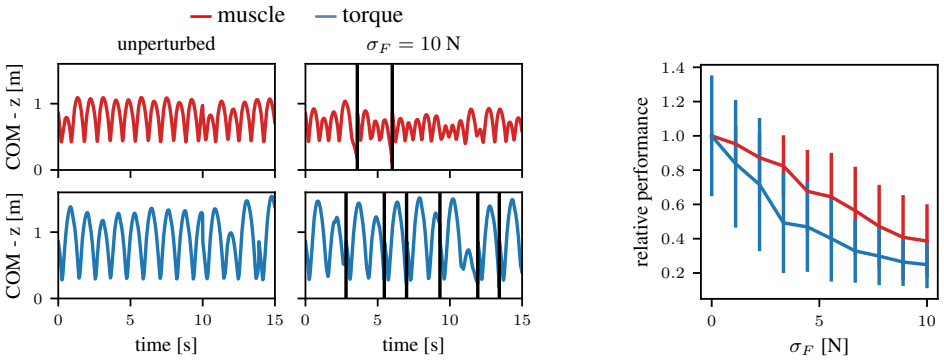

Figure 9: **Muscle actuators lead to more robust hopping.** At each time step, there is a 5 % chance of a random force being applied to the hip, knee, and ankle joints. Left: COM motion over time. Vertical bars mark episode resets due to falls of the Biped. Right: Relative performance for different standard deviations of the random force σ_F. Performance is scaled by the unperturbed mean return.

and high-jumping. In bipedal hopping, it was found that muscles result in more efficient learning, even though some torque-runs achieve higher asymptotic performance. Finally, we observe muscle actuation to result in increased robustness to perturbations and hyperparameter variations, which can facilitate learning on real robotic systems that not only present sensor and motor noise, but also prohibit extensive parameter searches.

To harness these biological properties, artificial muscles can be directly built as hardware [22, 37, 23, 38] or virtually implemented through software [39]. In particular, the muscle implementation that we apply to the MuJoCo models can efficiently create muscle-like behavior in real-time, which might be used to induce virtual muscle actuation in real systems, provided a sufficient control frequency.

Limitations Although we have reported results for a wide variety of algorithms and tasks, we cannot give theoretical statements about the general applicability of our findings. Additionally, some of the tasks we employed were limited in complexity and might also be solvable with classical control algorithms. The MuJoCo muscle model, while computationally efficient, only captures rudimentary properties of biological systems. The demoa implementation, on the other hand, includes visco-elastic, passive tendon characteristics and muscle routing as joint angle-dependent lever arms to account for many physiological details—at substantial additional computational cost. Finally, learning with intermediate control signals given to impedance or position controllers, instead of direct torque commands, might also improve learning performance, while muscle-like properties could have been introduced by learning priors or additional cost terms.

References

[1] H. Wagner and R. Blickhan. Stabilizing function of skeletal muscles: an analytical investigation. *Journal of Theoretical Biology*, 199(2):163–179, 1999.

[2] M. Eriten and H. Dankowicz. A rigorous dynamical-systems-based analysis of the self-stabilizing influence of muscles. *Journal of Biomechanical Engineering*, 131(1):011011, 2009.

[3] S. Brändle, S. Schmitt, and . Müller, Matthias A. Mathematical Biology A systems-theoretic analysis of low-level human motor control : application to a single-joint arm model. *Journal of Mathematical Biology*, 11 2019. doi:10.1007/s00285-019-01455-z.

[4] K. Stollenmaier, W. Ilg, and D. F. B. Haeufle. Predicting Perturbed Human Arm Movements in a Neuro-Musculoskeletal Model to Investigate the Muscular Force Response. *Frontiers in Bioengineering and Biotechnology*, 8(308), 4 2020. doi:10.3389/fbioe.2020.00308.

[5] A. J. van Soest and M. F. Bobbert. The contribution of muscle properties in the control of explosive movements. *Biological Cybernetics*, 69(3):195–204, 1993.

[6] D. Haeufle, S. Grimmer, and A. Seyfarth. The role of intrinsic muscle properties for stable hopping - stability is achieved by the force-velocity relation. *Bioinspiration & Biomimetics*, 5 (1):016004, 2010. doi:10.1088/1748-3182/5/1/016004.

[7] K. G. Gerritsen, A. J. van den Bogert, M. Hulliger, and R. F. Zernicke. Intrinsic muscle properties facilitate locomotor control—a computer simulation study. *Motor control*, 2(3): 206–220, 1998.

[8] C. T. John, F. C. Anderson, J. S. Higginson, and S. L. Delp. Stabilisation of walking by intrinsic muscle properties revealed in a three-dimensional muscle-driven simulation. *Computer methods in biomechanics and biomedical engineering*, 16(4):451–462, 2013.

[9] R. J. Full and D. E. Koditschek. Templates and anchors: neuromechanical hypotheses of legged locomotion on land. *Journal of Experimental Biology*, 202(23):3325–3332, 1999.

[10] P. Holmes, R. J. Full, D. Koditschek, and J. Guckenheimer. The dynamics of legged locomotion: Models, analyses, and challenges. *SIAM review*, 48(2):207–304, 2006.

[11] R. Blickhan, A. Seyfarth, H. Geyer, S. Grimmer, H. Wagner, and M. Günther. Intelligence by mechanics. *Philosophical Transactions of the Royal Society A: Mathematical, Physical and Engineering Sciences*, 365(1850):199–220, 2007.

[12] D. Haeufle, M. Günther, G. Wunner, and S. Schmitt. Quantifying control effort of biological and technical movements: an information-entropy-based approach. *Physical Review E*, 89(1): 012716, 2014.

[13] D. F. Haeufle, I. Wochner, D. Holzmüller, D. Driess, M. Günther, and S. Schmitt. Muscles reduce neuronal information load: quantification of control effort in biological vs. robotic pointing and walking. *Frontiers in Robotics and AI*, 7:77, 2020.

[14] F. Fischer, M. Bachinski, M. Klar, A. Fleig, and J. Müller. Reinforcement learning control of a biomechanical model of the upper extremity. *Scientific Reports*, 11(1):14445, July 2021. doi:10.1038/s41598-021-93760-1.

[15] E. Joos, F. Péan, and O. Goksel. Reinforcement learning of musculoskeletal control from functional simulations. In *International Conference on Medical Image Computing and Computer-Assisted Intervention*, pages 135–145. Springer, 2020.

[16] V. Caggiano, H. Wang, G. Durandau, M. Sartori, and V. Kumar. Myosuite – a contact-rich simulation suite for musculoskeletal motor control, 2022. URL https://arxiv.org/abs/2205.13600.

[17] P. Schumacher, D. Häufle, D. Büchler, S. Schmitt, and G. Martius. Dep-rl: Embodied exploration for reinforcement learning in overactuated and musculoskeletal systems, 2022. URL https://arxiv.org/abs/2206.00484.

[18] V. L. Barbera, F. Pardo, Y. Tassa, M. Daley, C. Richards, P. Kormushev, and J. Hutchinson. OstrichRL: A musculoskeletal ostrich simulation to study bio-mechanical locomotion. In *Deep RL Workshop NeurIPS 2021*, 2021. URL https://arxiv.org/abs/2112.06061.

[19] Ł. Kidziński, S. P. Mohanty, C. F. Ong, Z. Huang, S. Zhou, A. Pechenko, A. Stelmaszczyk, P. Jarosik, M. Pavlov, S. Kolesnikov, et al. Learning to Run challenge solutions: Adapting reinforcement learning methods for neuromusculoskeletal environments. In *The NIPS'17 Competition: Building Intelligent Systems*, 2018. URL http://arxiv.org/abs/1804.00361.

[20] Ł. Kidziński, C. Ong, S. P. Mohanty, J. Hicks, S. Carroll, B. Zhou, H. Zeng, F. Wang, R. Lian, H. Tian, et al. Artificial Intelligence for Prosthetics - challenge solutions. 2019. URL http://arxiv.org/abs/1902.02441.

[21] S. Song, Ł. Kidziński, X. B. Peng, C. Ong, J. Hicks, S. Levine, C. G. Atkeson, and S. L. Delp. Deep reinforcement learning for modeling human locomotion control in neuromechanical simulation. *Journal of NeuroEngineering and Rehabilitation*, Aug 2021.

[22] D. Driess, H. Zimmermann, S. Wolfen, D. Suissa, D. Haeufle, D. Hennes, M. Toussaint, and S. Schmitt. Learning to control redundant musculoskeletal systems with neural networks and sqp: exploiting muscle properties. In *2018 IEEE International Conference on Robotics and Automation (ICRA)*, pages 6461–6468. IEEE, 2018.

[23] D. Büchler, R. Calandra, and J. Peters. Learning to control highly accelerated ballistic movements on muscular robots. *Robotics and Autonomous Systems*, 2019.

[24] T. Siebert and C. Rode. Computational modeling of muscle biomechanics. In *Computational Modelling of Biomechanics and Biotribology in the Musculoskeletal System*, chapter 6, pages 173–204. Woodhead Publishing, Elsevier, 1 edition, 2014.

[25] R. Rockenfeller, M. Günther, S. Schmitt, and . Götz, Thomas. Comparative sensitivity analysis of muscle activation dynamics. *Computational and Mathematical Methods in Medicine*, 2015: 1–16, 2015. doi:10.1155/2015/585409.

[26] S. Schmitt. demoa-base: A Biophysics Simulator for Muscle-driven Motion, 2022. URL https://doi.org/10.18419/darus-2550.

[27] E. Todorov, T. Erez, and Y. Tassa. MuJoCo: A physics engine for model-based control. In *2012 IEEE/RSJ International Conference on Intelligent Robots and Systems*, pages 5026–5033, Oct. 2012. doi:10.1109/IROS.2012.6386109.

[28] N. Hansen, S. D. Müller, and P. Koumoutsakos. Reducing the time complexity of the derandomized evolution strategy with covariance matrix adaptation (cma-es). *Evolutionary computation*, 11(1):1–18, 2003.

[29] M. J. Powell. The bobyqa algorithm for bound constrained optimization without derivatives. *Cambridge NA Report NA2009/06, University of Cambridge, Cambridge*, 26, 2009.

[30] A. Abdolmaleki, J. T. Springenberg, Y. Tassa, R. Munos, N. Heess, and M. Riedmiller. Maximum a posteriori policy optimisation. In *International Conference on Learning Representations*, 2018. URL https://arxiv.org/abs/1806.06920.

[31] F. Pardo. Tonic: A deep reinforcement learning library for fast prototyping and benchmarking. 2020. URL https://arxiv.org/abs/2011.07537.

[32] I. Wochner and S. Schmitt. arm26: A Human Arm Model, 2022. URL https://doi.org/10.18419/darus-2871.

[33] I. Wochner, D. Driess, H. Zimmermann, D. F. Haeufle, M. Toussaint, and S. Schmitt. Optimality principles in human point-to-manifold reaching accounting for muscle dynamics. *Frontiers in Computational Neuroscience*, 14:38, 2020.

[34] J. R. Walter, M. Günther, D. F. Haeufle, and S. Schmitt. A geometry-and muscle-based control architecture for synthesising biological movement. *Biological Cybernetics*, 115(1):7–37, 2021.

[35] J. R. Walter, I. Wochner, M. Jacob, K. Stollenmaier, P. Lerge, and S. Schmitt. allmin: A Reduced Human All-Body Model, 2022. URL https://doi.org/10.18419/darus-2982.

[36] M. G. Pandy, F. E. Zajac, E. Sim, and W. S. Levine. An optimal control model for maximum-height human jumping. *Journal of Biomechanics*, 23(12):1185–1198, 1990.

[37] S. Wolfen, J. Walter, M. Günther, D. F. Haeufle, and S. Schmitt. Bioinspired pneumatic muscle spring units mimicking the human motion apparatus: benefits for passive motion range and joint stiffness variation in antagonistic setups. In *2018 25th International Conference on Mechatronics and Machine Vision in Practice (M2VIP)*, pages 1–6. IEEE, 2018.

[38] A. Volchko, S. K. Mitchell, T. G. Morrissey, and J. S. Humbert. Model-based data-driven system identification and controller synthesis framework for precise control of siso and miso hasel-powered robotic systems. In *2022 IEEE 5th International Conference on Soft Robotics (RoboSoft)*, pages 209–216, 2022. doi:10.1109/RoboSoft54090.2022.9762220.

[39] F. J. Abu-Dakka and M. Saveriano. Variable impedance control and learning—a review. *Frontiers in Robotics and AI*, 7:590681, 2020.